Architecture
Image Studies

Vol.7, Issue 1, pp.1353-1371, 2026
DOI: https://doi.org/10.62754/ais.v7i1.1028

https://journals.ap2.pt/index.php/ais/index

Energy Performance Assessment of the Deanship Building Under Three HVAC Systems: A Comparative Case Study

Shimaa H Saadoon[1], Omer M. Hamdoon[2], Reem A. Alothman[3]

Abstract

HVAC systems represent the largest proportion of energy consumption in buildings, necessitating the analysis and evaluation of alternative technologies to achieve energy efficiency and sustainability. This study analyzes and compares the thermal and energy performance of three common air conditioning systems used in building applications: Variable Refrigerant Flow (VRF) systems, Air-cooled Chiller systems, and packaged DX system. The thermal simulation software Design Builder was used to model the behavior of these three systems Inside the Deanship building of the College of Engineering at the University of Nineveh in Mosul, under continuous climatic conditions. Two types of simulations were performed for the building at different WWR ratios (10, 20, 30, 40, 50, 60) %. The addition of (XPS Extruded Polystyrene - CO2 Blowing) type insulation to the walls and roofs with a thickness of (1, 2, 3, 4, 5, 6) centimeters was also tested. In all these cases, the building's energy consumption was tested using the above systems. The summer simulation of the (cooling load) for air conditioning systems was conducted from (20 June to 22 September), while the winter simulation of the (heating load) was conducted from (21 December to 20 March). Results showed that VRF systems achieved energy savings of 50% in summer and 60% in winter compared to Air-cooled Chiller System, VRF systems also achieved savings of 18% in summer and 15% in winter compared to Packaged DX System.

Keywords: *HVAC, Energy Performance, Variable Refrigerant Flow (VRF) systems, Variable Air Volume (VAV) systems, packaged DX system, Simulation.*

Introduction

Background

The construction sector consumes the largest share of energy globally, with HVAC systems accounting for a significant portion, representing up to 60% of total building energy consumption [1]. In a country like Iraq, specifically in Mosul, harsh climatic conditions pose significant challenges during the summer and winter months, this places immense pressure on the national power grid due to the intensive use of air conditioning systems. University buildings, such as the Deanship office of the College of Engineering at the University of Nineveh, as an example of buildings requiring precise thermal management due to their occupancy patterns and the heavy use of office equipment. The Deanship building of the College of Engineering at the University of Nineveh consists of seven floors and has an area of approximately 7000 square meters, this building was chosen for this study. These buildings must provide a comfortable thermal environment for employees and visitors. Selecting the optimal air conditioning system remains a challenge for engineers and decision-makers, as an unsuitable choice leads to energy waste and increased operating costs. With advancements in engineering tools, Design Builder has emerged as one of the most powerful engineering simulation programs used to simulate building performance and evaluate the systems used within them. This research aims to conduct an analytical study comparing the performance of three air conditioning systems, it is (VRF) systems, Air-cooled Chiller systems, and packaged DX system, and evaluating their energy consumption during the summer and winter months in the College of Engineering building

[1] Department of Mechanical Engineering, College of Engineering, University of Mosul, Mosul, Iraq., E-mail address: shimaa.23enp@student.uomosul.edu.iq (Corresponding Author)
[2] Department of Sustainable Energy Engineering, College of Engineering, University of Mosul, Mosul, Iraq..
[3] Department of Architectural Engineering, College of Engineering, University of Mosul, Mosul, Iraq.

at the University of Nineveh. The study seeks to identify the most efficient system suitable for Mosul's climatic conditions.

Nomenclature:			
a – f	Curve fitting coefficients for HVAC performance curves	*Greek symbols*	
CAPFT	Capacity modifier curve (function of temperature)	η	Efficiency (Motor or Isentropic)
COP	Coefficient of Performance		
Cp	Specific heat of air		
CR	Combination Ratio (Indoor/Outdoor capacity ratio)		
EIRFPLR	Energy Input Ratio as a function of Part-Load Ratio		
H	Latent heat of vaporization		
M	Mass flow rate of air		
P	Power consumption (Compressor or Fan)	*Subscripts*	
PEQ	Equivalent piping length		
PH	Vertical height difference of piping	ref coil coil	Reference condition Cooling or heating coil
PLR	Part-Load Ratio		
Q avail	Available cooling capacity		
Q total	Total cooling capacity (sensible + latent)		
Q sens	Sensible cooling capacity		
Q lat	Latent cooling capacity		
SHR	Sensible Heat Ratio		
Tcond	Entering air dry-bulb temperature for condenser		
T cw Tin Twb *w*	Leaving chilled water temperature Inlet air temperature Entering air wet-bulb temperature Humidity ratio		

Literature Review

Numerous studies have been conducted to compare the performance of HVAC systems in buildings:

Studies conducted by several researchers, including Xinqiao Yu et al [2], BYONGMO SEO [3], Tolga N. et al [4] have shown that Variable Refrigerant Flow (VRF) systems achieve savings of up to 70% compared to Variable Air Volume (VAV) systems, in addition to being more efficient at low and medium loads. Study [5], conducted by Xiaobing Lin and Tianzhen Hong, indicated that Ground source heat pump (GSHP) systems may outperform VRF systems in cold climates such as Chicago. Study by R.parameshwaran and others [6] implemented a VAV-TES system in India, achieving energy savings of up to 47% compared to conventional systems. Intelligent control in Study [7], conducted by Prashant Anand et al of a VAV system in Singapore resulted in energy savings ranging from 19% to 38%. In another context, Study by Yonghua ZHU et al [8] presented a hybrid VRF/VAV control strategy that resulted in an additional 5.17% energy savings. Study by M. M.S. Dezfouli et al. [9], conducted in

Malaysia to evaluate the efficiency of an FCU system in a school building, showed that the average monthly consumption reached 1360.3 kWh. Another study by M.M.S. Dezfoli et al in Malaysia [10] found that 52% of the total heat load is related to latent loads and 48% to sensible loads. Regarding building envelope characteristics, several studies have been conducted. Study by Raad Z. Homod et al [11] compared modern and traditional building materials and showed that mud buildings are 47.83% more energy-efficient than concrete buildings. Study by Elisabeth Kossecka and Jan Kosny [12] also confirmed that a large wall mass improves thermal performance. A study by Abdul Hamid Al Abdul Jabbar et al conducted in Saudi Arabia [13] showed that neglecting roof insulation contributed to a 44.7% increase in heat load. Study by Zu-An Liu et al [14] indicated that insulating exterior walls improved energy efficiency. Regarding windows, studies by Aiman Mohammed et al [15], and Andre Feliks Setiawan et al [16] confirmed that the use of external shading and window breakers significantly reduced the heat load. Studies by Qiaoxia Yang et al [17], and Seok-Gil Yong et al [18]

This research will contribute to identifying methods for reducing energy consumption in educational buildings in Iraq.

showed that increasing the heat load window-to-wall ratio (WWR) increases annual energy consumption. Study by Ahmed Abdullah et al [19], demonstrated that the west-facing side of the building recorded the highest cooling load, while the northwest-facing side recorded the lowest.

Statement of Contribution

The aim of this research is to analyze and compare the performance of three HVAC systems in a specific building and to identify the most energy-efficient and providing thermal comfort to the user. This study is conducted in an administrative building in Mosul, where this type of study has not been previously conducted in Mosul.

Methodology

Building Description

The building where thermal analysis of the systems used and thermal simulations are being performed using Design Builder software is the Engineering Deanship building at the University of Nineveh. This building is currently under construction and is located in Mosul, Nineveh Governorate, which has a continental climate with hot summers and cold winters. These climatic conditions significantly affect the building's thermal loads. To give realistic results for Mosul's climate, the weather file in epw format was used and to set timetables that reflect the actual occupancy pattern of the Deanship from 8:00 am to 3:00 pm. See Tables 1,2,3.

Table 1. Location and Climate Characteristics.

Parameter	Description
Geographic location	Mosul District, Nineveh Governorate, Iraq
Latitude	36.34° N
Longitude	43.13° E
Building status	Under construction

Table 2. Summary of Building Construction Materials and Assemblies.

Building Element	Material Composition
Exterior Walls	Concrete block; cement mortar; internal plaster; external finishing layer; polyethylene insulation.
Interior Walls	Cement mortar; hollow concrete block; internal plaster finish.
Ceilings	Gypsum; cement; concrete blocks; gypsum board; air layer; polyethylene insulation.

Roof (Fifth Floor)	Outer exposed surface of the building constructed using the ceiling assembly materials.
Floors	Cement; sand; gravel; ceramic tiles.
Glazing System	Single glazing; double glazing; glass in various colors.

Table 3. Summary of Floor Layouts.

Floor Level	Description	Floor Area (m^2)	WWR Default %
Base Floor	7 rooms	580	30.00
Ground Floor	14 rooms; includes public facilities and reception halls	1975	30.00
First Floor	22 rooms	1775	30.00
Second Floor	18 rooms	1360	30.00
Third Floor	24 rooms	1280	30.00
Fourth Floor	18 rooms	905	30.00
Fifth Floor	Roof level/ outer exposed surface	108	30.00

The HVAC Systems Used in the Building

VRF, DOAS system: Variable refrigerant flow (VRF), also known as variable refrigerant volume (VRV), is an HVAC technology invented by Daikin Industries, Ltd. in 1982. Similar to ductless mini-split systems, VRFs use refrigerant as the primary cooling and heating medium, and are usually less complex than conventional chiller-based systems [20].

VAV (air cooled chiller, reheat): This type of system consists of: An air handling unit to cool or heat the air. A VAV box containing supports that control airflow. Fans to circulate air through the system. Temperature sensors to measure room temperature and adjust airflow. Reheat units to heat the air when needed [21].

Packaged DX System: The DX system works by transferring heat between the refrigerant and water or air without a medium, and its components are as follows:

1. Evaporator: This section absorbs heat from the surrounding environment and converts the refrigerant into vapor.

2. Compressor: This section raises the temperature of the vapor by increasing its pressure.

3. Condenser: Due to the heat generated by the high pressure, this section converts the vapor back into a liquid.

4. Expansion System: This section introduces the liquid into the evaporator and reduces its pressure, thus completing the system cycle [22].

Modeling with Design Builder

This section will explain the steps before conducting the simulation, which are as follows:

1. Building the building model in Design Builder version (7.0.2.006).: This involves importing the building model as a 2D plan from AutoCAD. Each floor is imported individually and converted into a 3D model within Design Builder. After completing all the floors, they are combined to form a complete building consisting of a base floor, a ground floor, and five additional floors. The building's orientation and geographical location are then determined.

2. Building the walls: After the three-dimensional building model is completed using the design builder program, the interior and exterior walls are built, and their composition, number of layers, and specifications of these layers are determined according to Table 4, which shows Wall layers and thickness, and Table 5. shows the U value of the wall at each insulation thickness value.

3. Building the roofs: The external roofs and the roofs between floors are built roof by roof, and their layers and the specifications of each layer. Table 6, which shows roof layers and thickness, Table 7, shows the U value of the roof at each insulation thickness value.

4. Building the openings (doors and windows): After completing the walls and ceilings, the doors and windows are built and their specifications are entered.

5. Enter the activities of the building's occupants and the equipment used in it, along with defining the building's usage schedules by its occupants.

6. Build the lighting system, including its type, number, and intensity: where the type of lighting system is selected within the building.

7. Enter the parts and data numbers of the air conditioning systems.

8. Configure the pre-simulation settings of the fixed and variable inputs and manage the simulation.

Table 4. Wall Layers and Thickness

layer name	Layer thickness (cm)
Cement/plaster/mortar /cement	3
concrete block (heavyweight)	20
Perlite plastering	3

Table 5. The U Value of the Wall At Each Insulation Thickness Value

insulation thickness (cm)	U value of wall (w/m2-k)
0	2.443
1	0.997
2	0.771
3	0.628
4	0.53
5	0.459
6	0.404

Table 6. Roof Layers and Thickness.

layer name	Layer thickness (cm)
Ceramic/porcelain	1
Cement/plaster/mortar /plaster	2
Cast concrete (Dense)	20
Gypsum plastering	2

Table 7. The U Value of The Roof at Each Insulation Thickness Value.

insulation thickness (cm)	U value of roof (w/m2-k)
0	2.515
1	1.445
2	1.014
3	0.781
4	0.635
5	0.535
6	0.462

The figures below show the building's floors in AutoCAD and Design Builder format:

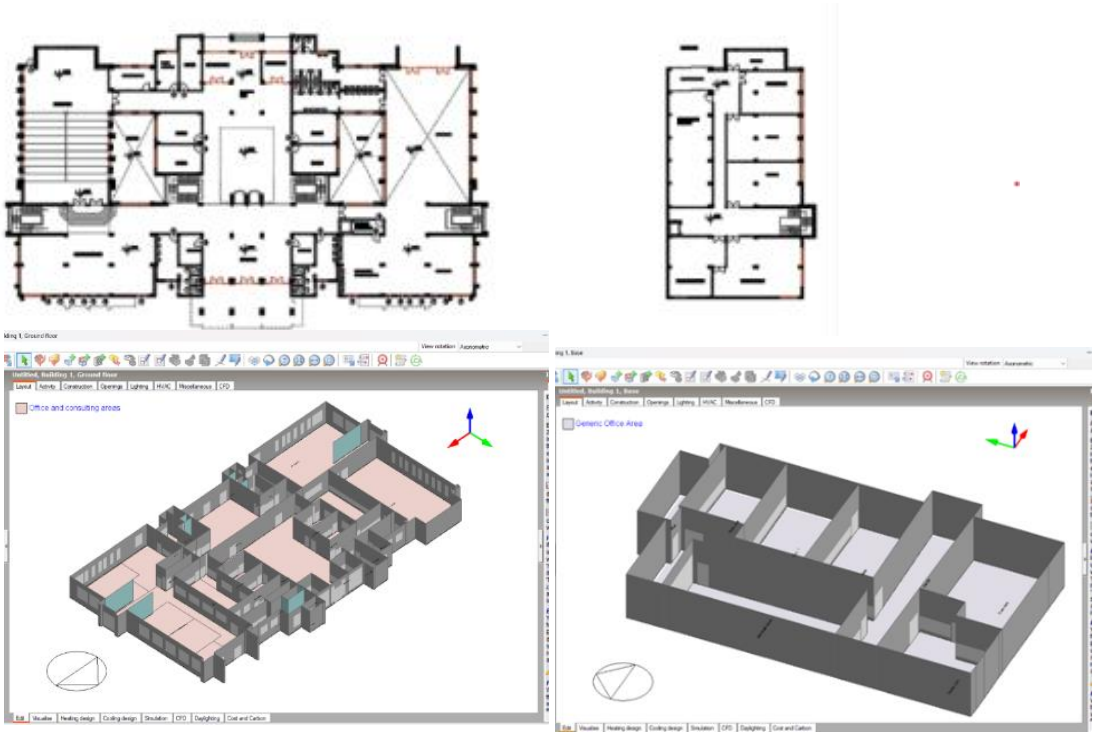

Figure 1. Base and ground floor plans by AutoCAD and Design Builder

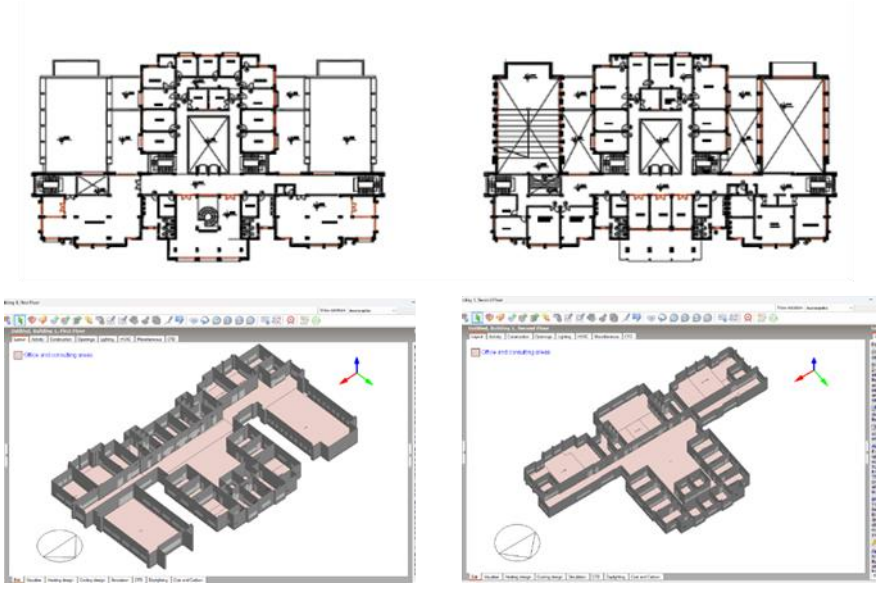

Figure 2. First and second-floor plans by AutoCAD and Design Builder.

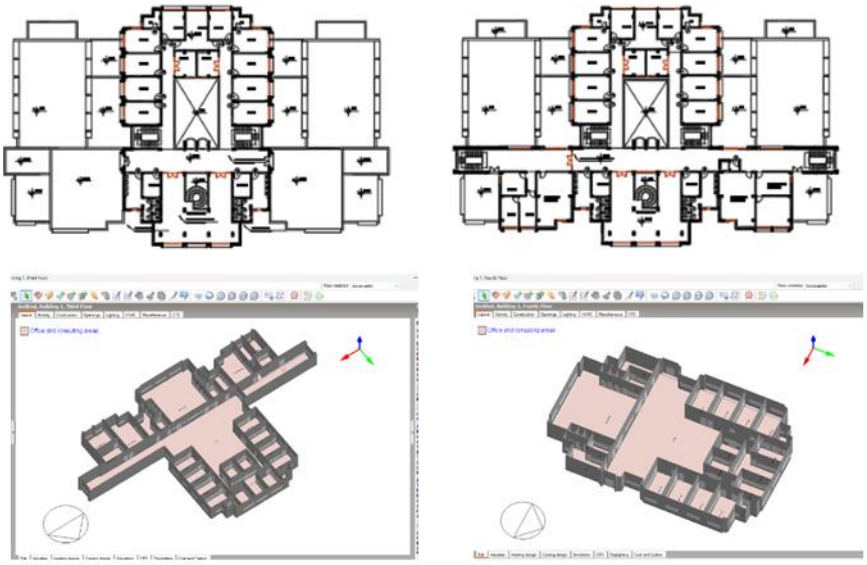

Figure 3. Third and fourth-floor plans by AutoCAD and Design Builder.

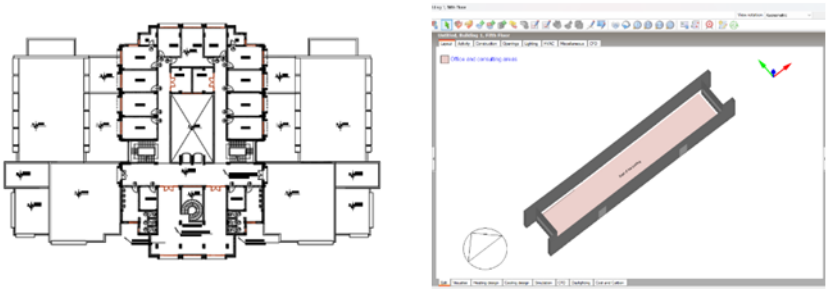

Figure 4. fifth floor plan by AutoCAD and Design Builder.

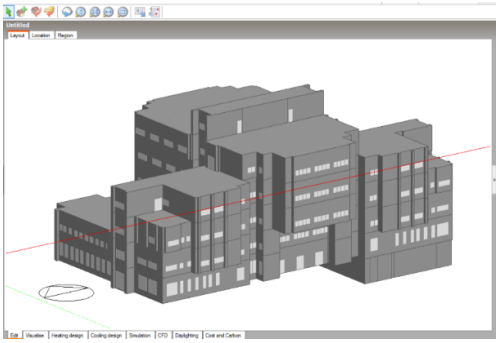

Figure 5. The entire building shape by Design Builder.

As for the three types of air conditioning systems used in the study, Fig. 6 shows each of them within the design builder program:

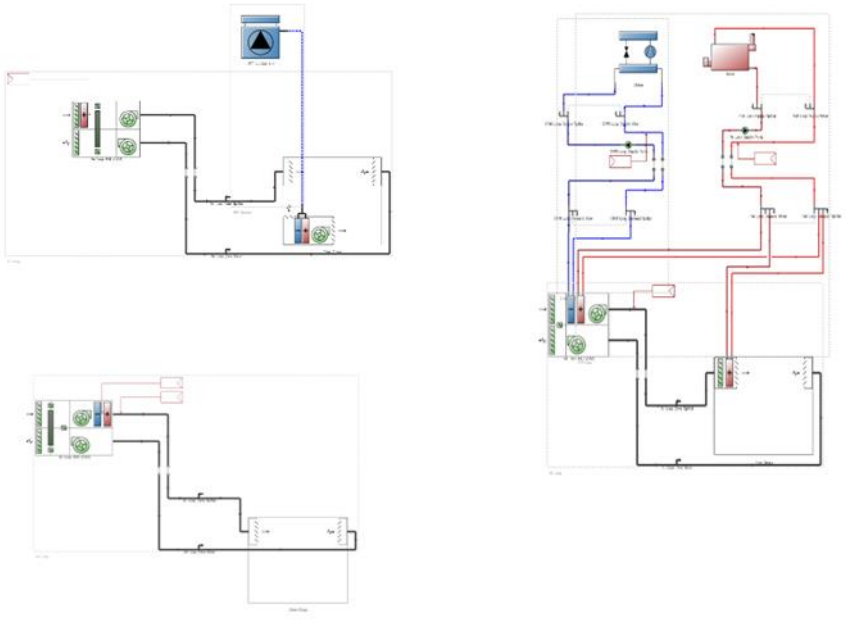

Figure 6. shows the three systems Variable Refrigerant Flow (VRF) systems, Air-cooled Chiller systems, and packaged DX system in order.

Model Setup

After the model was completed, and to achieve the objectives of this study in analyzing and evaluating the performance of the previously identified air conditioning systems, the simulator was applied to the seven-story Deanship building. The building simulation relied on several factors, including the selection of Mosul's climate data, which is based on the Mosul Energy Plus Weather (EPW) profile and standard climatic year (TMY) data. The performance of the three air conditioning systems was then simulated and analyzed using the detailed air conditioning technique in the Design Builder software. The weekly occupancy pattern is five working days (Sunday to Thursday), with Friday and Saturday being official holidays. Between 8:00 AM and 3:00 PM, occupancy rates gradually increase, reaching its peak between 9:00 AM and 1:00 PM. This simulation includes studying the effect of several variables on the overall building load and on the performance of specific HVAC systems. The first change is changing the window area on the walls, where WWR values of 10, 20, 30, 40, 50, and 60% were used for both summer and winter conditions. The hypothetical building scenario involves a structure with no wall or ceiling insulation and single-pane windows. The effect of this ratio on the building's daily energy consumption is then studied for both summer and winter. In another change, the same WWR values were used with roller blinds, and their impact on the building's load and daily energy consumption was examined and compared to the scenario without roller blinds for both summer and winter. Finally, the same WWR values were used with 1 cm thick wall insulation. The second simulation used wall insulation, with thickness values of 1, 2, 3, 4, 5, and 6 centimeters for each type of air conditioning system. The following Table 8 shows the variables that change during the simulation process.

Table 8. Shows The Parameters That Change During the Simulation Process.

Parameters	**Limits of change**
Thickness of insulation material	(1,2,3,4,5,6) cm
WWR	(10,20,30,40,50,60) %
Air conditioning units used	Air-cooled Chiller System, VRF System, Packaged DX System.
Daily simulation period	20 June to 22 September 21 December to 20 March

Mathematical Framework for Simulation

Design Builder uses algorithms to solve equations that represent the thermal behavior of the building, represented by the following equations:

VRF system modeling: governing equations of VRF system [23]:

The operating capacity of the Dx-cooler for the peripheral unit can be calculated as follows:

$$CAPFT_{coil,cooling} = a + b(\mathrm{T_{wb,i}}) + c(\mathrm{T_{wb,i}})^2 + d(\mathrm{T_c}) + e(\mathrm{T_c})^2 + f(\mathrm{T_{wb,i}})(\mathrm{T_c}) \quad (1)$$

Where;

$CAPFT_{coil,cooling}$ = zone coil Cooling Capacity Ratio Modifier (function of temperature), $\mathrm{T_{wb,i}}$= wet-bulb temperature of the air entering the cooling coil in zone I (°C), a–f = equation coefficients for Cooling Capacity Ratio Modifier, Tc = temperature of the air entering an air-cooled or evaporatively-cooled condenser (°C), [23].

The sensing capacity of a cooling coil is defined as the total capacity of the cooling coil multiplied by the sensing temperature ratio of the coil under current operating conditions, and is calculated as follows:

$$\dot{Q}_{\mathrm{coil(i),Cooling,total}} = \dot{Q}_{\mathrm{coil(i),Cooling,rated}}(CAPFT_{coil,cooling}) \quad (2)$$

$$PLR_i = 1 \quad (3)$$

$$SHR_{PLR} = f(\mathrm{T_{wb,i}} PLR_i, \dot{m}_{\mathrm{i}})$$

Where;

$\dot{Q}_{\mathrm{coil(i),Cooling,total}}$ = zone terminal unit total (sensible + latent) cooling capacity, [W], $\dot{Q}_{\mathrm{coil(i),Cooling,sensible}}$ = zone terminal unit sensible cooling capacity [W], PLR_i = cooling coil sensible part-load ratio in zone I, SHR_{PLR} = cooling coil sensible heat ratio (function of PLR, inlet air wet-bulb temperature, and cooling coil inlet air mass flow rate), $\dot{m}_{\mathrm{i}}$= cooling coil inlet air mass flow rate [m3/s], [23].

$$P_{correction,cooling} = a + b(P_{EQ,cooling}) + c(P_{EQ,cooling})^2 + d(CR_{cooling}) + e(CR_{cooling})^2 + f(P_{EQ,cooling})(CR_{cooling}) + g(P_H) \quad (6)$$

Where;

$P_{correction,cooling}$ = Piping Correction Factor in Cooling Mode, a – f = equation coefficients for piping correction factor in cooling mode, g = user specified piping correction factor for height in cooling mode coefficient, $P_{EQ,cooling}$= user specified equivalent piping length in cooling mode [m], $CR_{cooling}$ = combination ratio in cooling mode (total rated indoor terminal unit capacity divided by the rated condenser cooling capacity) (reported to eio file), P_H = user specified vertical height used for piping correction factor calculation [m], [23].

The total demand for the heat pump condenser is calculated as the quotient of the total cooling capacity of the terminal unit divided by the cooling pipe correction factor, as follows:

$$\dot{Q}_{\mathrm{cooling,total}} = \frac{\dot{Q}_{\mathrm{cooling,TerminalUnits}}}{P_{correction,cooling}} \quad (7)$$

the available cooling capacity in heat recovery mode will be:

$$\dot{Q}_{\mathrm{HR,Cooling,total}} = \dot{Q}_{\mathrm{HP,Cooling,total}}(HRC_{ap}\, Mod_{HP,cooling}) \quad (8)$$

Where;

$\dot{Q}_{\mathrm{HR,Cooling,total}}$ = heat recovery total available cooling capacity (W).

The partial operational load of the VRF system can then be calculated as follows:

$$PLR = \frac{\dot{Q}_{\mathrm{Cooling,total}}}{\dot{Q}_{\mathrm{HR,avail,Cooling}}} \quad (9)$$

Chiller system modeling: governing equations of Chiller system [24]:

When calculating the partial load ratio of an absorption chiller evaporator, the following equation is applied:

$$\text{PLR} = \frac{\dot{Q}_{\text{evap}}}{\dot{Q}_{\text{evap,rated}}} \quad (10)$$

where;
PLR is the part-load ratio of chiller evaporator, Q ̇_evapis the chiller evaporator load [W], $\dot{Q}_{\text{evap,rated}}$ is the rated chiller evaporator capacity [W].
The electrical energy used for the steam and pump is calculated as follows:

$$\text{Cycling Frac} = \text{Min}(1, \frac{\text{PLR}}{\text{PLR}_{\text{min}}}) \quad (11)$$

To calculate the cooling capacity based on temperature, use the following equation, this represents the ratio of energy input to temperature EIR F Temp):

$$\text{Cool Cap F Temp} = a + b(\text{T}_{\text{cw,ι}}) + c(\text{T}_{\text{cw,ι}})^2 + d(\text{T}_{\text{cond,}e}) + e(\text{T}_{\text{cond,}e})^2 + f(\text{T}_{\text{cw,ι}})(\text{T}_{\text{cond,}e}) \quad (12)$$

Where;
$T_{cw,l}$: Leaving chilled water temperature (°C), $T_{cond,e}$: Entering air dry-bulb temperature for air-cooled condensers (°C).

The available cooling capacity can be calculated using the following equation:

$$\dot{Q}_{avail} = \dot{Q}_{ref} \cdot \text{CoolCapFTemp} \quad (13)$$

Based on the partial load, the percentage of energy input can be calculated as follows:

$$\text{EIRFPLR} = a + b(PLR) + c(PLR)^2 \quad (14)$$

The cooling compressor's power is calculated using the following equation:

$$P_{chiller} = \dot{Q}_{avail} \cdot \left(\frac{1}{COP_{ref}}\right) \cdot \text{EIRFTemp} \cdot \text{EIRFPLR} \cdot \text{CyclingFrac} \quad \ldots \quad (15)$$

To calculate the power of a condenser fan, the following equation is used:

$$P_{cond,fan} = \dot{Q}_{ref} \cdot (P_{condfanratio}) \cdot \text{CyclingFrac} \quad \ldots (16)$$

Where;
P_condfanratio is fan power ratio (W/W).
To balance the heat ejected from the system, the following equation is applied:

$$\dot{Q}_{cond} = P_{chiller} \cdot \eta_{motor} + \dot{Q}_{evap} + \dot{Q}_{falseloading} \quad \ldots \quad (17)$$

Where;
η_{motor} is compressor motor efficiency.

Package DX System modeling: governing equations of Package DX System [25]:
The system calculates the sensible cooling load based on the temperature difference between the coil inlet and outlet point, as follows:

$$T_{\text{out,target}} = T_{\text{setpoint}} + (T_{\text{out,current}} - T_{\text{control,current}}) \quad (18)$$

the sensible cooling load is calculated using the following equation

$$Q_{\text{sens,load}} = \dot{m} \cdot c_p \cdot (T_{\text{in}} - T_{\text{out,target}}) \quad (19)$$

where;
$\dot{m}$ is the air mass flow rate and c_p is the specific heat of air.
The reasonable partial load ratio is calculated by comparing the load to the coil capacity as follows:

$$\text{PLR}_{\text{sensible}} = \max\left(0.0, \frac{Q_{sens,load} - Q_{no\ load}}{Q_{full\ load} - Q_{no\ load}}\right) \quad (20)$$

where;
$Q_{\text{full load}}$ = coil sensible cooling output at PLR = 1.0, $Q_{\text{no load}}$ = sensible cooling output with the coil OFF (fan only, if continuous).

To calculate the latent load, the following humidity ratios are used:

$$Q_{\text{lat,load}} = \dot{m} \cdot h_{fg} \cdot (w_{\text{in}} - w_{\text{setpoint}}) \quad (21)$$

Where;
h_{fg} is the latent heat of vaporization and w is humidity ratio.
The latent part-load ratio is calculated as:

$$\text{PLR}_{\text{latent}} = \min\left(\text{PLR}_{\text{min}}, \frac{w_{\text{in}} - w_{\text{setpoint}}}{w_{\text{in}} - w_{\text{out,HXon}}}\right) \quad (22)$$

where;
PLR_{min} is the minimum PLR for dehumidification (often 0.0), and $w_{\text{out, H Xon}}$ is the outlet humidity ratio when the coil (or heat exchanger) is active.

The percentage of operational partial load adjustment is greater than among PLRs and PLR latent as follows:

$$\text{PLR}_{\text{operating}} = \max(PLR_{sensible}, PLR_{latent}) \quad (23)$$

Results and Discussion

Building Energy Analysis

After simulating based on the identified factors (window-to-wall ratio, wall insulation, roof insulation, and the addition of roller blinds), and studying the impact of changing these factors on the daily load rate in summer and winter, as well as on the building's total energy consumption, the results were obtained for the heat gain rate through the building envelope and the total daily load required for cooling or heating in summer and winter. These simulations were conducted on January 16 and July 16, 2025. The results are plotted to illustrate the impact of the aforementioned factors on the hourly heat gain rate through the building envelope and on the total heat gain, as well as the impact of these factors on the heat loss rate through the roofs and walls and on the total heat loss.

Fig. 7 shows that the rate of heat gain through the building envelope increases as the ratio of windows to the wall increases in summer, due to the increased amount of heat transferred to the building through radiation falling on the windows, even though they reduced the uninsulated wall. For example, when the WWR percentage increased from 10% to 20%, the energy consumption rate increased from 118 kW to 139 kW, and when the percentage increased to 60%, the consumption rate reached 232 kW. As for Fig. 8 shows that the total heat gain through the building envelope increases per hour as the ratio of windows to walls increases, due to the increased area of glass exposed to the falling radiation, which leads to a rise in temperature inside the building. For example, the total heat load gained increased from 945 kWh to 1839 kWh when the WWR percentage increased from (10 to 60) %.

Fig. 9 shows that the rate of heat loss decreases when insulation is added to the roofs, and the greater the thickness of the insulation, the lower the heating load required for the building, and therefore the rate of energy consumption decreases. Adding 1 cm of insulation to the roofs reduced the average heat loss through the building envelope from 38.76 kW to 15.81 kW. This is because the insulation material prevents heat leakage from inside the building to the outside. As for Fig. 10 shows that the total building load decreases when insulation is added to the roofs because the insulation material prevents heat leakage from inside the building to the outside, where the total heat loss from the building decreased from 304.39 kWh to 124.226 kWh with the addition of 1 cm of insulation. The thicker the insulation, the lower the total load needed to heat the building, and therefore the lower the energy consumption.

Fig. 11, shows that the rate of heat gain decreases when insulation is added to the walls, and the greater the thickness of the insulation, the lower the rate of heat gain, thus reducing the cooling load required for the building. For example, when walls are insulated with a thickness of one centimeter, the heat gain rate decreases from 65.57 kW (without insulation) to 30.3 kW with one centimeter of insulation. Fig. 12, shows that the total energy consumption of the building decreases when insulation is added to the walls, for example, the total heat gain across the building envelope decreases from 523 kWh (without insulation) to 242 kWh with one centimeter of wall insulation, because the insulation reduces heat transfer into the building, thus maintaining a comfortable temperature inside and reducing the cooling load required for the building.

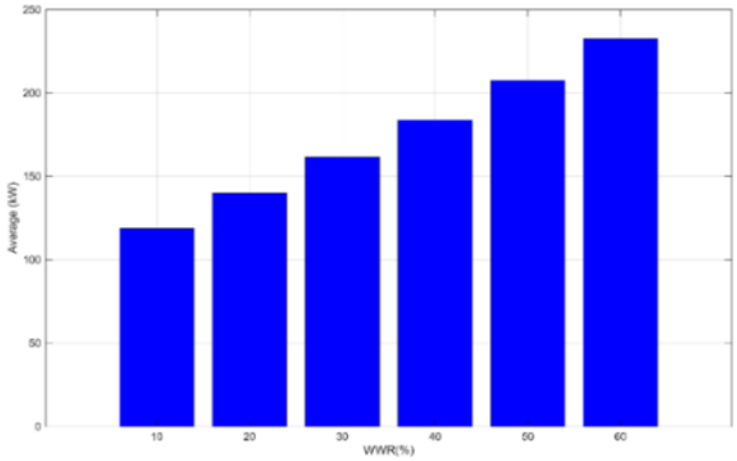

Figure 7. Average Hourly Heat Gain through the Building Envelope on 16 July 2025 at Different WWR (Uninsulated Walls).

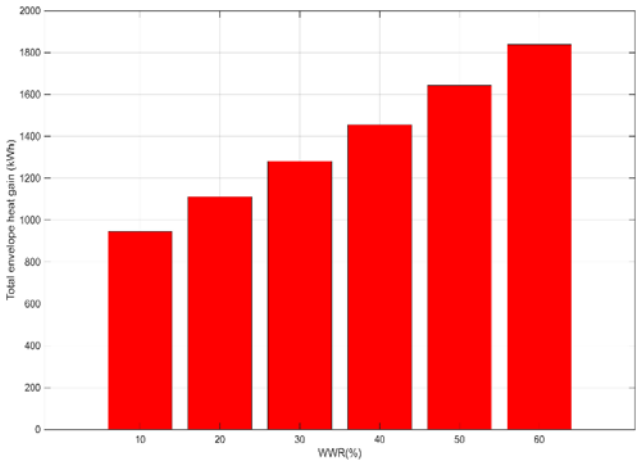

Figure 8. Total Envelope Heat Gain through the Building Envelope on 16 July 2025 at Different WWR (Uninsulated Walls).

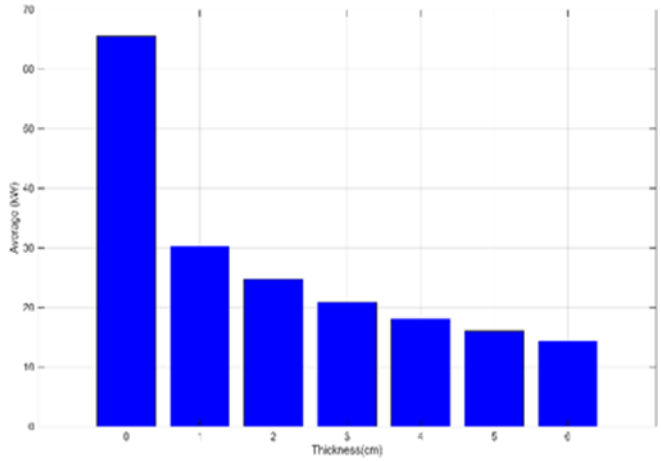

Figure 9. average Heat Loss Rate through Roof and Celling on 16 January 2025 at Different Insulation Thicknesses.

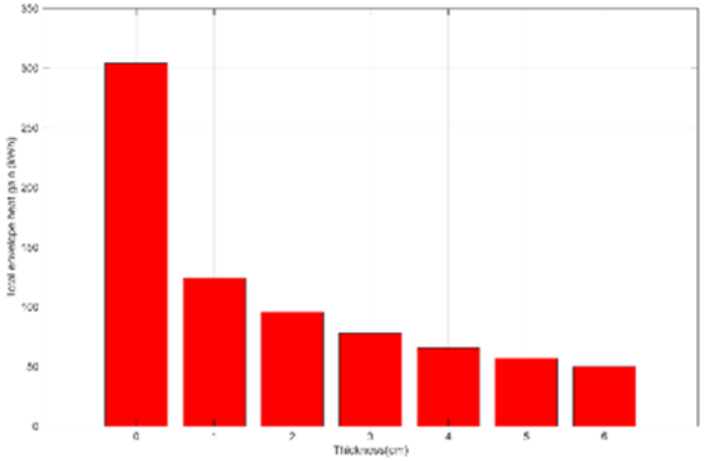

Figure 10. total Envelope Heat Loss Rate through Roof and Celling on 16 January 2025 at Different Insulation Thicknesses.

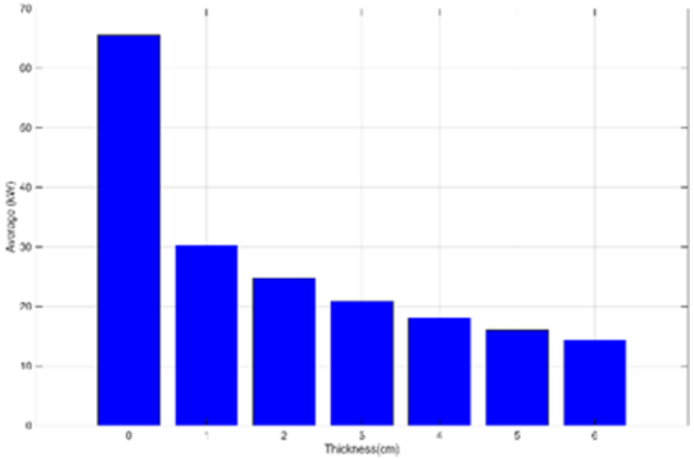

Figure 11. average Heat Gain Rate through Exterior Walls on 16 July 2025 at Different Insulation Thicknesses.

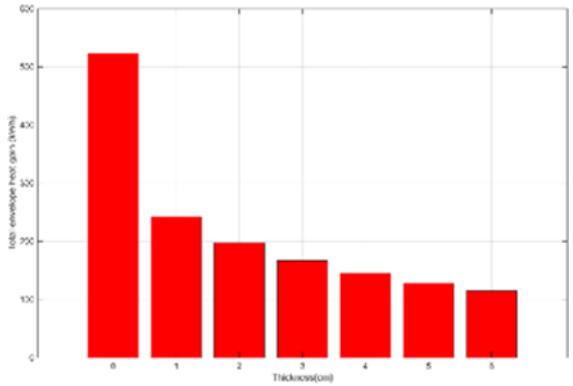

Figure 12. Total Envelope Heat Gain Rate through Exterior Walls on 16 July 2025 2025 at Different Insulation Thicknesses.

Comparative Performance of HVAC Systems

After conducting the simulation using the design builder software to evaluate the actual energy consumption resulting from the use of the previously specified air conditioning systems for the building, the results were as follows:

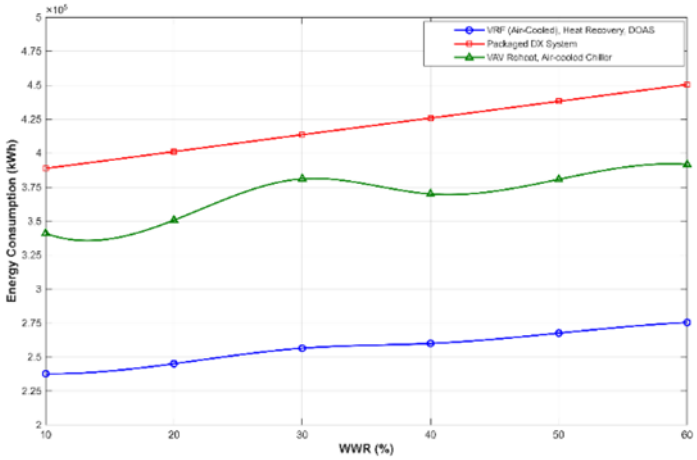

Figure 13. Effect of WWR on Summer HVAC Energy Consumption for Different HVAC Systems.

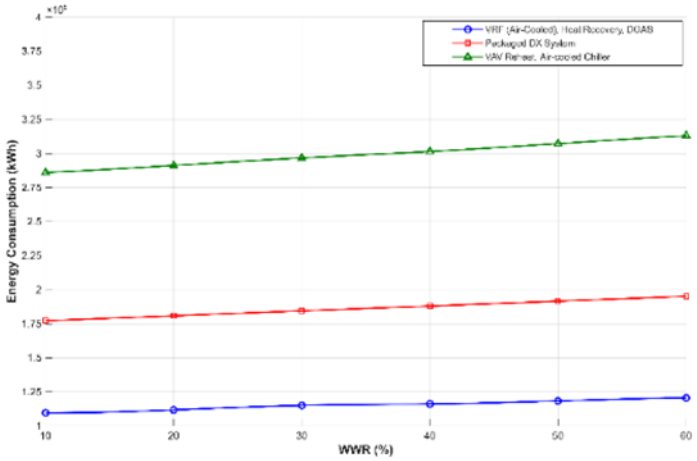

.

Figure 14. Effect of WWR on winter HVAC Energy Consumption for Different HVAC Systems.

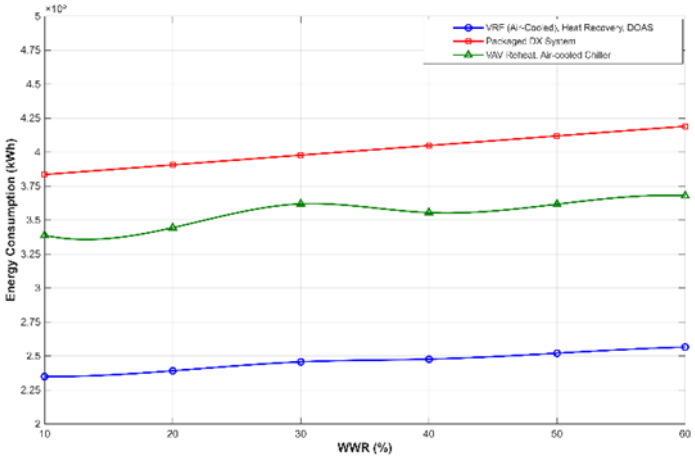

Figure 15. Effect of WWR on Summer HVAC Energy Consumption for Different HVAC Systems with Roller Shades.

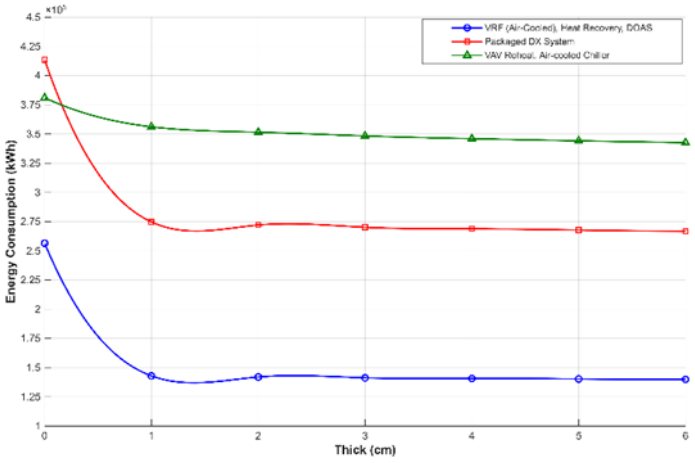

Figure 16. Effect of Wall Insulation Thickness on Summer HVAC Energy Consumption for Different HVAC Systems.

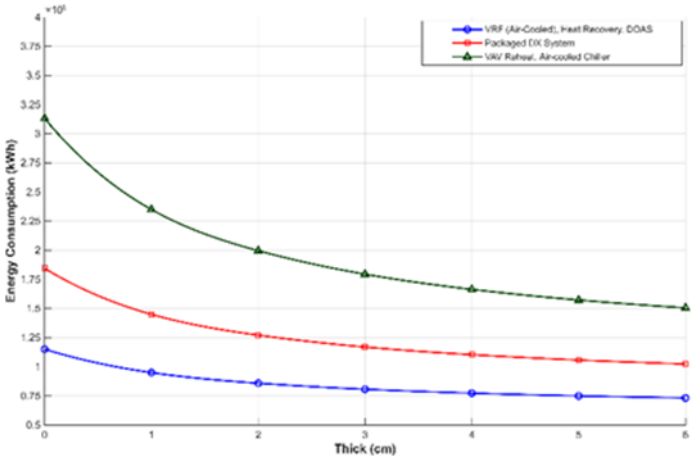

Figure 17. Effect of Wall Insulation Thickness on Winter HVAC Energy Consumption for Different HVAC Systems.

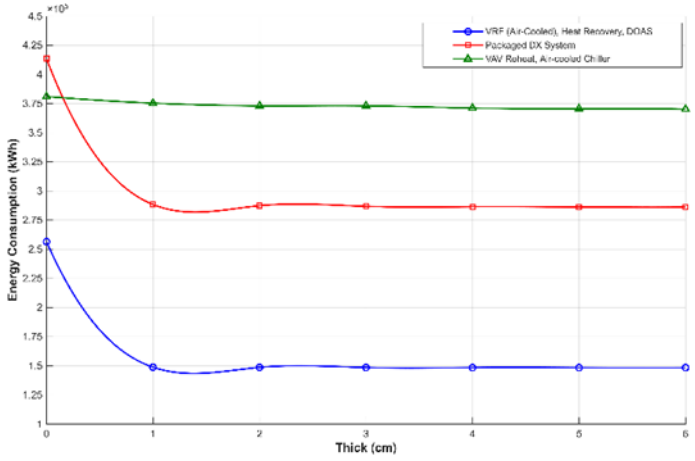

Figure 18. Effect of Roof Insulation Thickness on Summer HVAC Energy Consumption for Different HVAC Systems.

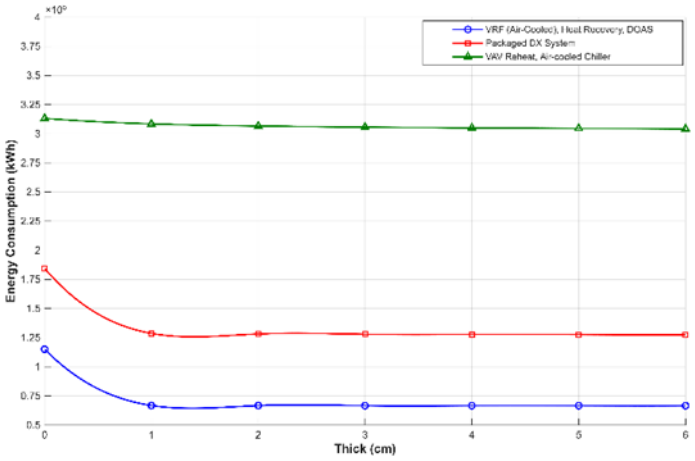

Figure 19. Effect of Roof Insulation Thickness on Winter HVAC Energy Consumption for Different HVAC Systems.

Discussion of the Results

Fig. 13, shows that increasing the window-to-wall ratio in summer leads to increased energy consumption for cooling the building across all three systems used. This is due to the increased surface area of glass exposed to incident solar radiation, resulting in greater heat transfer into the building and a rise in its temperature. By observing the curves, the DX system has a high energy consumption. For example, at WWR = 30%, the energy consumption of this system reached approximately 413,000 kwh, while the VRF system recorded the lowest consumption value, reaching 256,000 kwh.

Fig. 14, shows that increasing the WWR percentage in winter led to a slight increase in the energy consumption required to heat the building for all three systems, but less so than in summer. This is due to the reduced impact of daytime solar radiation and increased heat loss from inside the building to the outside. The figure indicates that the VRF system is the most efficient, the VAV system, on the other hand, was the least efficient. For example, at a WWR of 40%, The energy consumption by the VAV system reached approximately 301,000 kWh, while the energy consumption by the VRF system was 116,000 kWh. The DX system recorded an energy consumption between the two previous values for the same WWR value, which was 188,000 kWh. Therefore, the VRF system was the least energy-consuming for all WWR ratios.

Fig. 15, shows that increasing the ratio of windows to walls of the building in the summer, with the use of roller blinds and without insulation. For example, when comparing the energy consumption values of the three systems at WWR = 40% and with the curtains, the consumption values were VRF = 247,000 kWh, VAV = 355,000 kWh, and DX = 404,000 kWh approximately. From observing these values, the VRF system is the most efficient in energy consumption. When comparing with Fig. 13 at a

value of WWR = 40% and without the curtains, the energy consumption values were as follows: VRF = 260,000 kWh, VAV = 369,000 kWh, and DX = 425,000 kWh. Therefore, adding the roller curtains led to a reduction in the energy consumption of the three systems, as the VRF system was the best in both cases.

In Fig. 16, It can be observed the effect of adding insulation to the building walls at different insulation thicknesses during the summer. Adding 1 cm thick polystyrene insulation significantly reduced energy consumption for all three systems used to cool the building, as it prevented heat transfer into the building. For example, the energy consumption of the VRF system decreased from 256,515.63 kWh without insulation to 142,914.83 kWh with only 1 cm of insulation, while the VAV system was the most energy-intensive, and with the same insulation thickness of one centimeter, the consumption was 356,000 kilowatt-hours. We also observe that the effect of increasing insulation thickness diminishes gradually, and this effect becomes particularly noticeable when moving from no insulation to insulation with a thickness of 1 cm. Furthermore, the VRF system is the most efficient among the systems used, recording the lowest energy consumption at all insulation thickness levels.

Fig. 17, shows that adding insulation to the building walls reduces heat loss from the inside of the building to the outside during winter, thus lowering the energy consumption required for heating. For example, with 1 cm of insulation, the energy consumption of the VRF system decreased from 115,115 kWh to 95,000 kWh, while the energy consumption of the VAV system decreased from 313,000 kWh to 235,000 kWh. We observe that the VRF system has the lowest energy consumption across all insulation thickness values, while the energy consumption of the VAV and DX systems decreases, but remains high compared to the VRF system. The VAV system recorded the highest energy consumption; for example, with 6 cm of insulation thickness, the VRF system consumed 73,000 kWh, the DX system 102,000 kWh, and the VAV system 150,000 kWh.

Fig. 18, illustrates the effect of adding insulation to the roof on summer energy consumption for the three systems. We observe that switching from no insulation to 1 cm thick insulation resulted in a significant reduction in energy consumption for cooling the building. This is because the roof is the part most exposed to direct solar radiation for extended periods. Furthermore, the VRF system demonstrated high energy efficiency across all insulation thickness levels compared to the other systems. For example, when 1 cm of insulation was added, the VRF system recorded the lowest energy consumption at 148,000 kWh, the DX system at 288,000 kWh, and the VAV system at 375,000 kWh, the highest among these systems. These curves show that, across all insulation thickness values, the VRF system is the most energy-efficient, Meanwhile, the VAV system remains the most energy-intensive.

Fig. 19, illustrates the effect of roof insulation on the energy consumption of the three systems used to heat the building in winter. Adding insulation significantly reduces energy consumption. For example, for a VRF system without insulation, consumption decreased from 115,115 kWh to 66,779 kWh with 1 cm of insulation. While the VAV system is the least affected by the addition of insulation due to its reliance on reheating units, which consume a large amount of energy in winter to maintain comfortable temperatures inside the building. Where consumption decreased from 313,000 kWh to 308,000 kWh, while the DX system recorded a decrease from 184,000 kWh to 128,000 kWh. Therefore, the VAV system was the most energy-intensive despite the addition of insulation to the ceilings.

Conclusions

Through dynamic simulations conducted on the Deanship building of the College of Engineering at the University of Nineveh, the research reached the following conclusions:

It concludes from Fig. 13 that the VRF system, compared to the VAV system, achieves energy savings of up to 44%, and compared to the DX system, it achieves energy savings of up to 15% in the summer in the case of increasing the ratio of windows to walls and without insulation

From Fig. 14, we can conclude that the VRF system achieves energy savings in winter in the case of increasing the ratio of windows to walls and without insulation

of up to 60% compared to the VAV system, while it achieves savings of up to 10% compared to the DX system.

It concludes from Fig. 15 that the VRF system, compared to the VAV system, saves up to 45% of energy when using roller shades.

From Fig. 16, we can conclude that the VRF system's energy consumption decreased by 44% when 1 cm of wall insulation was added, saving 50% of energy compared to the VAV system under the same insulation conditions. It also saved 18% of energy compared to the DX system.

It concludes from Fig. 17 that the VRF system maintains an energy savings rate of up to 60% in winter when insulating walls compared to the VAV system and 15% compared to the DX system.

While it can be concluded from Fig. 18 that the VRF system is the most responsive to roof insulation in summer and provides up to 45% more energy compared to the VAV system and 20% compared to the DX system.

From Fig. 19, it can be concluded that the VRF system recorded energy savings of up to 65% compared to the VAV system when insulating one centimeter of the roof in winter and saved 12% compared to the DX system.

It turned out that roof insulation is more important than wall insulation due to its direct and prolonged exposure to solar radiation in Mosul.

The effect of increasing insulation thickness was gradual and not substantial, with the greatest impact observed when transitioning from no insulation to 1 cm of insulation

Recommendations

Based on the above, the research recommends the following:

Adopting the VRF system as a primary option when upgrading or designing air conditioning systems for University of Nineveh building due to its high efficiency in hot, dry, and cold climates.

It also recommends reducing the percentage of window area on facades exposed to the sun (south and west) in order to avoid high loads.

It is recommended to insulate the roofs of existing buildings with a thickness of no less than (3-5) centimeters because this step has the highest return in saving energy.

Conduct an economic feasibility study that includes the cost of purchasing and maintaining these systems and compare it with the savings resulting from this simulation.

References

[1] Review of energy-efficient HVAC technologies for sustainable buildings. (2024). 1–8. https://doi.org/10.53771/ijstra.2024.6.2.0039

[2] Yu, X., Yan, D., Sun, K., Hong, T., & Zhu, D. (2016). Comparative study of the cooling energy performance of variable refrigerant flow systems and variable air volume systems in office buildings. Applied Energy, 183, 725–736. https://doi.org/10.1016/j.apenergy.2016.09.033

[3] Seo, B., Yoon, Y. B., Yu, B. H., Cho, S., & Lee, K. H. (2020). Comparative analysis of cooling energy performance between water-cooled VRF and conventional AHU systems in a commercial building. Applied Thermal Engineering, 170. https://doi.org/10.1016/j.applthermaleng.2020.114992

[4] Aynur, T. N., Hwang, Y., & Radermacher, R. (2009). Simulation comparison of VAV and VRF air conditioning systems in an existing building for the cooling season. Energy and Buildings, 41(11), 1143–1150. https://doi.org/10.1016/j.enbuild.2009.05.011

[5] Liu, X., & Hong, T. (2010). Comparison of energy efficiency between variable refrigerant flow systems and ground source heat pump systems. Energy and Buildings, 42(5), 584–589. https://doi.org/10.1016/j.enbuild.2009.10.028

[6] Parameshwaran, R., Harikrishnan, S., & Kalaiselvam, S. (2010). Energy efficient PCM-based variable air volume air conditioning system for modern buildings. Energy and Buildings, 42(8), 1353–1360. https://doi.org/10.1016/j.enbuild.2010.03.004

[7] Anand, P., Sekhar, C., Cheong, D., Santamouris, M., & Kondepudi, S. (2019). Occupancy-based zone-level VAV system control implications on thermal comfort, ventilation, indoor air quality and building energy efficiency. Energy and Buildings, 204(December), 1–8. https://doi.org/10.1016/j.enbuild.2019.109473

[8] Aynur, T. N., Hwang, Y., & Radermacher, R. (2009). Simulation comparison of VAV and VRF air conditioning systems in an existing building for the cooling season. Energy and Buildings, 41(11), 1143–1150. https://doi.org/10.1016/j.enbuild.2009.05.011

[9] Dezfouli, M. M. S., Dehghani-Sanij, A. R., Kadir, K., Suhairi, R., Rostami, S., & Sopian, K. (2023). Is a fan coil unit (FCU) an efficient cooling system for net-zero energy buildings (NZEBs) in tropical regions? An experimental study on thermal comfort and energy performance of an FCU. Results in Engineering, 20(December), 1–46. https://doi.org/10.1016/j.rineng.2023.101524

[10] Dezfouli, M. M. S., Kadir, K., Dehghani-Sanij, A. R., Rostami, S., Suhairi, R., & Mohd Azmi, M. A. (2023). Thermal Comfort and Energy Analysis of Fan Coil Unit Cooling Systems in Tropical Buildings. 2023 International Conference on Engineering Technology and Technopreneurship, ICE2T 2023, 335–340. https://doi.org/10.1109/ICE2T58637.2023.10540541

[11] Homod, R. Z., Almusaed, A., Almssad, A., Jaafar, M. K., Goodarzi, M., & Sahari, K. S. M. (2021). Effect of different building envelope materials on thermal comfort and air conditioning energy savings: A case study in Basra city, Iraq. Journal of Energy Storage, 34(February), 1–11. https://doi.org/10.1016/j.est.2020.101975

[12] Kossecka, E., & Kosny, J. (2002). Influence of insulation configuration on heating and cooling loads in a continuously used building. Energy and Buildings, 34(4), 321–331. https://doi.org/10.1016/S0378-7788(01)00121-9

[13] Search, C., & Khusus, U. E. (2025). Zoom _ Out _ Map Search Menu Zoom _ Out _ Map. 1–29.

[14] Liu, Z. A., Li, Y., Hou, J., Tian, L., Wang, S., Hu, W., & Zhang, L. (2025). Impact of exterior envelope thermal performance on energy demand and optimization strategies for university teaching-office buildings. Scientific Reports, 15(1), 1–38. https://doi.org/10.1038/s41598-025-00045-y

[15] Search, C., & Khusus, U. E. (2025). Zoom _ Out _ Map Search Menu Zoom _ Out _ Map. 1–29.

[16] Setiawan, A. F., Huang, T. L., Tzeng, C. T., & Lai, C. M. (2015). The effects of envelope design alternatives on the energy consumption of residential houses in Indonesia. Energies, 8(4), 2788–2802. https://doi.org/10.3390/en8042788

[17] Yang, Q., Liu, M., Shu, C., Mmereki, D., Uzzal Hossain, M., & Zhan, X. (2015). Impact Analysis of Window-Wall Ratio on Heating and Cooling Energy Consumption of Residential Buildings in Hot Summer and Cold Winter Zone in China. Journal of Engineering (United Kingdom), 2015, 1–36. https://doi.org/10.1155/2015/538254

[18] Yong, S. G., Kim, J. H., Gim, Y., Kim, J., Cho, J., Hong, H., Baik, Y. J., & Koo, J. (2017). Impacts of building envelope design factors upon energy loads and their optimization in US standard climate zones using experimental design. Energy and Buildings, 141(April), 1–15. https://doi.org/10.1016/j.enbuild.2017.02.032

[19] Abdalla, A., Islam, M. D., & Janajreh, I. (2025). Influence of building orientation on cooling load: A comparative study. International Journal of Thermofluids, 27(May), 1–48. https://doi.org/10.1016/j.ijft.2025.101244

[20] Kim, J., CaraDonna, C., Parker, A. (2023). Variable Refrigerant Flow with Heat Recovery and Dedicated Outdoor Air System. National Renewable Energy Laboratory /TP-5500-86103.

[21] A. Bhatia, B.E. (2020). HVAC Design Overview of Variable Air Volume Systems.

[22] Cycle, T. R. (2023). ENGINEERS Understanding the Selection of Direct Expansion (DX) Coils for Both Cooling and Heating. 52(March), 1–8.

[23] Reference, E. (n.d.). Engineering Reference — Energy Plus 8.5 <<. 1–34.

[24] Reference, E. (n.d.). Chillers [LINK] Absorption Chiller [LINK]. 1–31.

[25] Engineers, A., Engineers, A., Technologies, I., Engineers, A., Claridge, D. E., Elliot, R. N., Shepard, M., Greenberg, S., Katz, G., Rise, P., & Engineers, A. (2008). 16.5.1 Unitary Systems. 1118–1192.